

## Supporting Information for

# Self-Assembly of Rod-Coil Block Copolymers on a Substrate into Micrometer-Scale Ordered Stripe Nanopatterns

Zhengmin Tang,<sup>a</sup> Da Li,<sup>a</sup> Jiaping Lin,<sup>\*,a</sup> Liangshun Zhang,<sup>a</sup> Chunhua Cai,<sup>\*,a</sup> Yuan Yao,<sup>a</sup> Chunming Yang,<sup>b</sup> and Xiaohui Tian<sup>a</sup>

<sup>a</sup>Shanghai Key Laboratory of Advanced Polymeric Materials, Key Laboratory for Ultrafine Materials of Ministry of Education, Frontiers Science Center for Materiobiology and Dynamic Chemistry, School of Materials Science and Engineering, East China University of Science and Technology, Shanghai 200237, China

<sup>b</sup>Shanghai Synchrotron Radiation Facility, Shanghai Advanced Research Institute, Chinese Academy of Sciences, Shanghai 201204, China

---

**\*Corresponding Author**

Tel: +86-21-6425-3370. E-mail: [jlin@ecust.edu.cn](mailto:jlin@ecust.edu.cn); [caichunhua@ecust.edu.cn](mailto:caichunhua@ecust.edu.cn)

## Content

1 Experimental and Simulation Methods .....	SI-3
1.1 Polymer Synthesis and Sample Preparation .....	SI-3
1.2 Characterizations .....	SI-6
1.3 Simulation Method .....	SI-8
2. Experimental and Simulation Results .....	SI-12
2.1 Self-Assembly of PBLG- <i>b</i> -PEG on PS-silicon Substrate. ....	SI-12
2.2 Thickness of the Thin Films on Substrate .....	SI-13
2.3 Self-Assembly of PBLG- <i>b</i> -PEG with Higher Molecular Weights on Substrate.....	SI-14
2.4 Self-Assembly of Rod-Coil Copolymers on Substrate Revealed by Simulations.....	SI-15
2.5 Aggregates Formed in Solutions at High Block Copolymer Concentrations.....	SI-17
2.6 Effect of Assembling Temperature on Surface Morphology .....	SI-18
2.7 Effect of THF/DMF Ratios and Temperatures on Surface Morphology .....	SI-19
2.8 Self-Assembly of PBLG- <i>b</i> -PEG on Various Substrates .....	SI-21
2.9 Effect of Rigidity of Rod Blocks on Formation of Ordered Nanopatterns .....	SI-23
2.10 Conventional Spin-Coating Approach. ....	SI-24

# 1 Experimental and Simulation Methods

## 1.1 Polymer Synthesis and Sample Preparation

**Reagents and materials.** Polystyrene (PS,  $M_n = 537 \text{ kg mol}^{-1}$ ,  $M_w/M_n = 1.03$ ), poly(methyl methacrylate) (PMMA,  $M_n = 501 \text{ kg mol}^{-1}$ ,  $M_w/M_n = 1.03$ ), and poly(2-vinylpyridine) (P2VP,  $M_n = 389 \text{ kg mol}^{-1}$ ,  $M_w/M_n = 1.12$ ) were purchased from Polymer Standards Service. Toluene (HPLC grade, > 99.9%),  $\alpha$ -Methoxy- $\omega$ -amino poly(ethylene glycol) (mPEG-NH<sub>2</sub>,  $M_n = 2$  or  $5 \text{ kg mol}^{-1}$ ) were purchased from Sigma-Aldrich.  $\gamma$ -Benzyl-L-glutamate-N-carboxyanhydride (BLG-NCA) was synthesized according to literature.<sup>S1, S2</sup> All other chemicals were obtained from Adamas-beta and purified according to conventional methods or used as received.

**Synthesis of PBLG-*b*-PEG block copolymers.** Poly( $\gamma$ -benzyl-L-glutamate)-*block*-poly(ethylene glycol)(PBLG-*b*-PEG) block copolymers were synthesized in anhydrous 1, 4-dioxane solution using ring-opening polymerization of BLG-NCA initiated by anhydrous mPEG-NH<sub>2</sub> macroinitiators.<sup>S2</sup> The monomer concentration was about 3.0 wt%. The reaction was performed in a flame-dried reaction bottle under a dry nitrogen atmosphere for 3 days at 15 °C. At the end of the polymerization, the reaction mixture was poured into a large volume of anhydrous ethanol. The precipitates were collected and dried under vacuum. The resulting products were purified twice by repeated precipitation from a chloroform solution into a large volume of anhydrous methanol.

The number-average molecular weight ( $M_n$ ) of the polypeptide blocks was estimated using <sup>1</sup>H NMR measurement (Avance 550, Nuclear, CDCl<sub>3</sub> as solvent) at room temperature. Since the  $M_n$  of the PEG block is known, the  $M_n$  of the PBLG block can be calculated by the peak intensity ratio of the methylene proton signal (5.1 ppm) of the PBLG to the ethylene proton signal (3.6 ppm) of the PEG (Figure S1a).<sup>S3</sup>

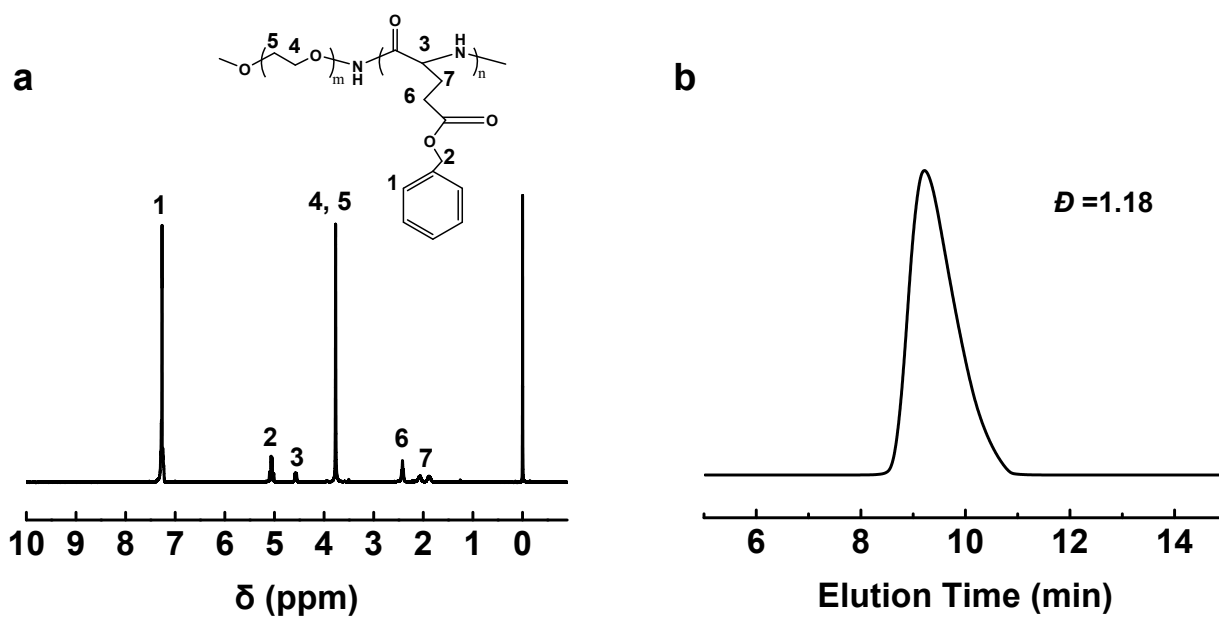


**Figure S1.** (a)  $^1\text{H}$  NMR spectrum of  $\text{PBLG}_{12\text{k}}\text{-}b\text{-PEG}_{5\text{k}}$  block copolymers in  $\text{CDCl}_3$ . (b) GPC trace of  $\text{PBLG}_{12\text{k}}\text{-}b\text{-PEG}_{5\text{k}}$  block copolymers.

**Table S1.** Characteristics of the block copolymers

Sample	$M_n$ ( $\text{kg mol}^{-1}$ ) <sup>a</sup>	$\text{DP}^a$	$\bar{D}^b$
$\text{PBLG}_{5\text{k}}\text{-}b\text{-PEG}_{2\text{k}}$	PEG: 2 PBLG: 5	PEG: 45 PBLG: 23	1.12
$\text{PBLG}_{8\text{k}}\text{-}b\text{-PEG}_{2\text{k}}$	PEG: 2 PBLG: 8	PEG: 45 PBLG: 37	1.21
$\text{PBLG}_{12\text{k}}\text{-}b\text{-PEG}_{5\text{k}}$	PEG: 5 PBLG: 12	PEG: 112 PBLG: 55	1.18
$\text{PBLG}_{20\text{k}}\text{-}b\text{-PEG}_{5\text{k}}$	PEG: 5 PBLG: 20	PEG: 112 PBLG: 91	1.21
$\text{PBLG}_{66\text{k}}\text{-}b\text{-PEG}_{5\text{k}}$	PEG: 5 PBLG: 66	PEG: 112 PBLG: 301	1.26

<sup>a</sup>Since the  $M_n$  value, and the degree of polymerization (DP) of the PEG segment are known, the  $M_n$  and DP of PBLG block were derived according to  $^1\text{H}$  NMR spectra.

<sup>b</sup>The  $\bar{D}$  values of the block copolymers were obtained from GPC testing.

The polydispersity index ( $\mathcal{D}$ ) of the block copolymers was measured by the gel permeation chromatography (PL-GPC, Varian, PBLG as standard) at 50 °C. As shown in Figure S1b, the GPC trace of the PBLG<sub>12k</sub>-*b*-PEG<sub>5k</sub> block copolymers displays monomodal distribution. The molecular characteristics of the block copolymers are provided in Table S1.

**Preparation of PS-silicon substrate.** The monodisperse PS homopolymers were dissolved in toluene with a concentration of ~2.5 wt%. Si (100) wafers with a native oxide layer (~2 nm), were cleaned by immersion in a hot piranha solution (*i.e.*, H<sub>2</sub>SO<sub>4</sub>:H<sub>2</sub>O<sub>2</sub>=3:1) for 30 min and rinsed with a great amount of deionized water and dried with a nitrogen gun. High-density and flattened PS nano-layers irreversibly adsorbed on Si substrates (PS-silicon substrate, stable in common solvents) were prepared according to literature.<sup>S4-S8</sup> Firstly, PS films were prepared by spin-coating dilute solutions of the polymer onto Si wafers. The spin-cast PS films were then annealed at about 160 °C for 3 days under vacuum below 10<sup>-3</sup> Torr. Afterward, the PS films were leached in baths of fresh toluene at room temperature until the resultant film thickness remained constant. Lastly, the resultant ultrathin PS films were dried in a vacuum oven at 70 °C for 12 h to remove any excess solvent trapped in the films before further experiments.

**Self-assembly of PBLG-*b*-PEG on PS-silicon substrate.** Firstly, the PBLG-*b*-PEG block copolymers were dissolved in THF/DMF mixtures. Then, 3 mL of the polymer solution was added to a beaker. Subsequently, a piece of Si-silicon wafer was immersed in a solution with the PS facing up. To avoid solvent evaporation, the beaker was then sealed. To induce the self-assembly of PBLG-*b*-PEG on the surface of PS-silicon, 1.2 mL of deionized water was added dropwise into the polymer solution with slightly stirring. The rate of water addition was *ca.* 100 μL/min, thus the self-assembly process can be completed within several minutes. Finally, the samples were rinsed with plenty of

water to quickly remove the organic solutions. The samples were dried in vacuum for 12 h before further characterization. For all the self-assembly experiments, polymer solutions, water for self-assembly, and water for rinsing were stored at corresponding temperatures for more than 12 h before use.

To examine the effect of block copolymer concentration on the assembled morphology, the experiments were conducted at various concentrations of 0.05 g L<sup>-1</sup>, 0.1 g L<sup>-1</sup>, 0.4 g L<sup>-1</sup>, 1.0 g L<sup>-1</sup>, respectively. The experimental temperature was fixed at 20 °C. To examine the effect of self-assembling temperature, the experiments were conducted at various temperatures of 20 °C, 25 °C, 30 °C, 35 °C, and 40 °C, respectively. The block copolymer concentration was fixed at 0.4 g L<sup>-1</sup>. To investigate the morphological evolution of the stripe nanopatterns, water was dropped quite slowly and the samples were incubated in solutions for more than 1 hour so that the equilibrium structures can be obtained at a certain water content.

## 1.2 Characterizations

**Atom Force Microscopy (AFM).** AFM images were obtained with an XE-100 AFM instrument (Park Systems), employing noncontact mode. To gain clear images, the images were set by 256 × 256 pixels, and a scan rate of 0.5 Hz was employed. The images were analyzed using professional software (XEI, Park Systems).

**Grazing-Incidence Small-Angle X-ray Scattering (GISAXS).** GISAXS experiments were performed at the Shanghai Synchrotron Radiation Facility (SSRF, China) BL16B beamline. The wavelength of the X-ray was 0.124 nm (E = 10 keV). The samples were placed on the sample stage, which can be translated in three directions and rotated around two orthogonal axes. To probe the surface and inner structure of the nanopatterns, for each sample, the X-ray incident angle was chosen

as  $0.3^\circ$  (above the critical angle). The exposure time was 100 s. The scattered intensity was collected on a 16-bit X-ray charge-coupled device ( $2048 \times 2048$  pixels, the pixel size of  $80 \times 80 \mu\text{m}^2$ ) placed at a distance of 1909 mm downstream from the sample. The direct incident beam and reflected beam were hidden by two-beam stops before the detector.

### 1.3 Simulation Method

**Dissipative particle dynamic (DPD) methods.** The dissipative particle dynamics (DPD) is a mesoscopic simulation method originated by Hoogerbrugge and Koelman,<sup>S9, S10</sup> developed by Robert and Patrick.<sup>S11</sup> In this method several neighboring molecules are grouped into a single particle. Newton's equations of motion are applied for the position-time relationship of every bead in the system. Using a modified velocity-Verlet algorithm, all beads' positions and velocities are integrated.

According to the DPD method, the force  $F_i$  applying on a coarse-grained DPD bead  $i$  is a sum of a conservative force, a dissipative force, and a random force, represented as the following equation

$$\mathbf{F}_i = \sum_{i \neq j} (\mathbf{F}_{ij}^C + \mathbf{F}_{ij}^D + \mathbf{F}_{ij}^R) \quad (\text{S-1})$$

The three kinds of forces on the right hand of the above equation take the forms as follows

$$\mathbf{F}_{ij}^C = \begin{cases} a_{ij} (1 - r_{ij} / r_c) \hat{\mathbf{r}}_{ij} & r_{ij} < r_c \\ 0 & r_{ij} \geq r_c \end{cases} \quad (\text{S-2})$$

$$\mathbf{F}_{ij}^D = \begin{cases} -\gamma (1 - r_{ij} / r_c)^2 (\hat{\mathbf{r}}_{ij} \cdot \mathbf{v}_{ij}) \hat{\mathbf{r}}_{ij} & r_{ij} < r_c \\ 0 & r_{ij} \geq r_c \end{cases} \quad (\text{S-3})$$

$$\mathbf{F}_{ij}^R = \begin{cases} (2\gamma k_B T)^{1/2} (1 - r_{ij} / r_c) \theta_{ij} (dt)^{-1/2} \hat{\mathbf{r}}_{ij} & r_{ij} < r_c \\ 0 & r_{ij} \geq r_c \end{cases} \quad (\text{S-4})$$

Here,  $a_{ij}$  is the repulsive parameter between two arbitrary beads  $i$  and  $j$ , and  $a_{ij} = 75k_B T / \rho + 3.27\chi_{ij}$ , where  $k_B$ ,  $T$ , and  $\chi_{ij}$  denotes to Boltzmann constant, temperature, and Flory-Huggins parameter, respectively.  $r_{ij}$  is the distance between these two beads  $r_{ij} = |\mathbf{r}_i - \mathbf{r}_j|$ ,  $\hat{\mathbf{r}}_{ij} = (\mathbf{r}_i - \mathbf{r}_j) / r_{ij}$  is the unit vector.  $r_c$  is the cutoff distance.  $\gamma$  is the strength of the dissipation between bead  $i, j$ , and  $\mathbf{v}_{ij} = \mathbf{v}_i - \mathbf{v}_j$  is relative velocity.  $\theta_{ij}$  is a random fluctuating variable with Gaussian statistics and has zero mean and unit deviation.

For the diblock copolymers, an additional harmonic spring potential  $U_{ij}^s = \frac{1}{2} k_s (r_{ij} - r_0)^2$  is applied to each pair of two bonded beads  $i$  and  $j$ . In this work, the equilibrium bond distance  $r_0$  and  $k_s$  are set to be  $0.7 r_c$  and  $100 k_B T / r_c^2$ , respectively. The rigidity of rod blocks is realized by cosine

harmonic function, which keeps the angle formed by every three beads to a constant value. The chain stiffness potential  $U_{ijk}^c = \frac{1}{2}k_c (\cos(\theta) - \cos(\theta_0))^2$  is performed on three neighbored beads  $i, j$ , and  $k$  in rod blocks. The equilibrium value of the angle  $\theta_0$  and the value of  $k_c$  are set as  $180^\circ$  and  $100 k_B T$ , respectively. Figure S2a shows the schematic illustration of the diblock copolymers model we constructed.

For simplicity, the polystyrene template was modeled to a planar substrate formed by beads (Figure S2b). The average distance between neighboring beads was set to close enough to avoid the copolymer and solvents permeating through the substrate. The simulations were performed in the  $l \times l \times h$  three-dimensional spaces with periodic boundary conditions and the size of the planar substrate is  $l \times l \times 1$ . The block copolymer beads and solvent beads with density  $\rho = 3$  were placed in the simulation box.

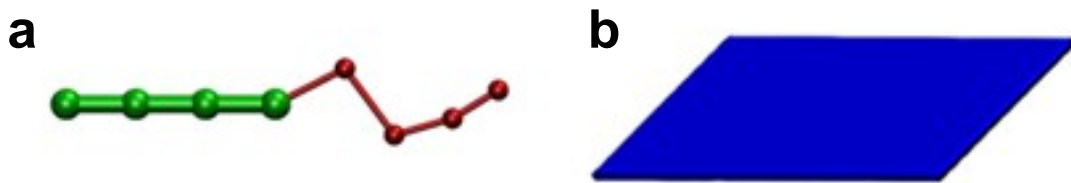


**Figure S2.** (a) The DPD model of amphiphilic rod-coil block copolymers (green beads stand for rigid hydrophobic rods, red beads stand for coiled hydrophilic block). (b) The model of a fixed planar substrate (blue).

Applying velocities with a Gaussian distribution to all the beads except those constructing the planar substrate, the DPD simulation method was then run for  $20000\tau$  to offer enough time for the systems reaching stable configurations. Under each parameter condition, the simulation was performed 10 times with different random number seeds, and the final quantitative results were averaged from all these 10 times simulations. The time step was set to  $\Delta t = 0.01\tau$ , in which

$\tau = \sqrt{mr_c^2 / (k_B T)}$ . The massive of all beads, cutoff distance, and temperature were all set unit ( $m = 1.0$ ,  $r_c = 1.0$  and  $k_B T = 1.0$ ), and the value of  $\tau$  was also assigned as a unit.

**Important parameters in simulation methods.** In the simulation, important parameters were set based on the experimental conditions. The followings are the discussion and explanation of the choice of these important parameters.

(1) **Bead number.** Keeping the total number of beads in the simulation box constant with density  $\rho = 3$ , the amount of block copolymer beads can be calculated as  $l^2 \times (h-1) \times \rho$  according to the sizes of the simulation box and the substrate. For simplicity, this value has been simplified to the surface density of copolymers ( $N/s$ ), where  $N$  denotes the number of diblock copolymer chains and  $s$  denotes the surface area of the planar substrate. The  $\mathbf{R}_4\mathbf{C}_4$  model of diblock copolymer constructed in the simulations corresponds to the PBLG<sub>12k</sub>-*b*-PEG<sub>5k</sub> in the experiments. The choice of the number of DPD beads in each rod block and coil block is based on our previous work and literature.<sup>S12, S13</sup> In the simulations, the mass of beads ( $m = 1$ ) and the bead distance/equilibrium bond length ( $0.7 r_c$ ) for different beads were fixed. The molecular weights of PBLG rod blocks and PEG coil blocks are 12000 and 5000, respectively. First, the number of DPD beads was renormalized by keeping the bulk density identical in the simulations and experiments, and then a ratio of 12000/5000 was obtained. In this work, 3.6 DPD beads for the PBLG form a 0.54 nm helix (or modeling rod), while 1 DPD bead for the PEG occupies 0.35 nm. Second, the number of DPD beads was renormalized by the length of rod blocks and coil blocks (the bead distance is equal to the equilibrium bond length), and we obtained the relative number of DPD beads for rod and coil blocks as  $(12000 \times 0.54 / 3.6) : (5000 \times 0.35 / 1) \approx 4.11 : 4$ . As a result, a model of  $\mathbf{R}_4\mathbf{C}_4$  rod-coil copolymers composed of 4 rod R beads and 4 coil C beads was adopted in the study.

(2) **The rigidity of molecules.** The PEG is flexible, thus only a bond potential was applied for the coil block in rod-coil copolymers. Since the PBLG homopolymers with  $\alpha$ -helix conformation are considered as rigid segments, in the simulations a bond-angle potential was employed to guarantee the rigidity of rod block by setting a large value of  $k_c = 100 k_B T$ .

(3) **Interaction parameter.** To facilitate a comparison with available experiments (PBLG-*b*-PEG/PS binary system in solvents), we set the interaction parameters  $a_{ij}$  in the DPD simulation close to those in experiment systems. For the beads of the same species, repulsive parameters were set as 25. The repulsive parameters between different types of beads were:  $a_{RC} = 80$ ,  $a_{RS} = 80$ ,  $a_{RP} = 25$ ,  $a_{CS} = 30$ ,  $a_{CP} = 25$ , and  $a_{PS} = 120$ . R, C, S, and P denote rod blocks (PBLG), coil blocks (PEG), solvents, and the beads constructing the planar substrate (PS), respectively. These parameters were set corresponding to the hydrophobicity of PBLG blocks and PS homopolymers and the hydrophilicity of PEG blocks. The value of  $a_{PS}$  was larger than the others to make sure the diblock copolymers attaching to the planar substrate without dissolving in the solvents.

## 2. Experimental and Simulation Results

### 2.1 Self-Assembly of PBLG-*b*-PEG on PS-silicon Substrate.

Figure S3 shows the typical AFM topographic images (from low to high magnifications) of the well-aligned stripe nanopatterns self-assembled from PBLG<sub>12k</sub>-*b*-PEG<sub>5k</sub> block copolymers on the PS-silicon substrate at 20 °C. As can be seen, the block copolymers cover the whole surface of the PS-silicon wafer and form well-aligned stripe nanopatterns. The ordered domain size of the nanopatterns can be up to 25 μm<sup>2</sup>, indicating that the adsorption and assembly of PBLG<sub>12k</sub>-*b*-PEG<sub>5k</sub> block copolymers on the substrate can produce large-area ordered nanostructures.

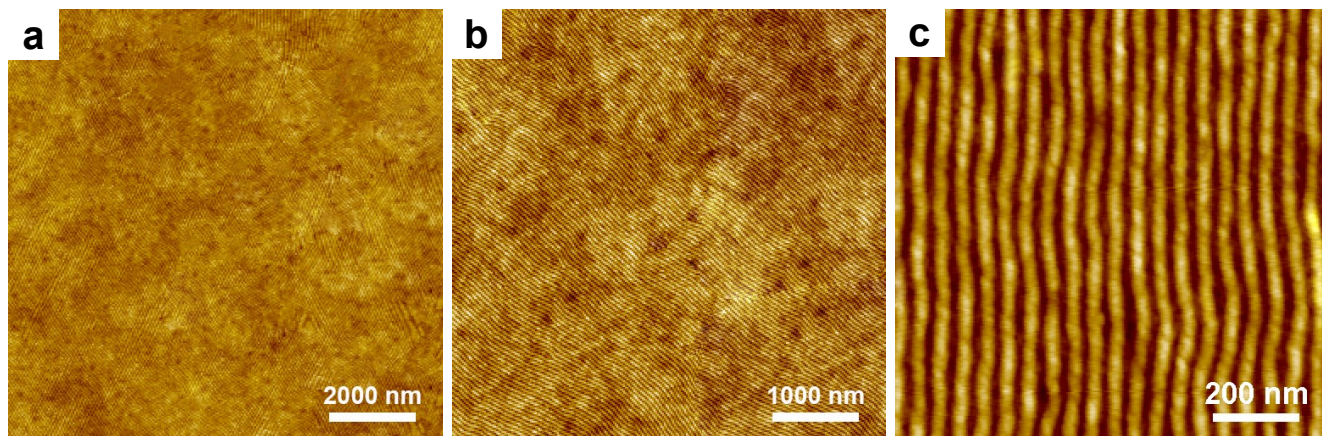


**Figure S3.** (a-c) AFM topographic images with various magnifications of the stripe nanopatterns self-assembled from PBLG<sub>12k</sub>-*b*-PEG<sub>5k</sub> block copolymers on the PS-silicon substrate.

## 2.2 Thickness of the Thin Films on Substrate

For the well-aligned stripe nanopatterns assembled on the PS-silicon substrate, we determined the thickness of the films via AFM measurements, considering the height of steps obtained by scratching parts of the organic layers off with a razor blade (Figure S4). The thickness of the spin-cast PS film and the flattened PS nano-layer were measured to be  $\sim 160$  nm and  $\sim 16$  nm, respectively (Figure S4a and S4b). The total thickness of PS nano-layer and stripe nanopatterns was measured to be  $\sim 22$  nm (Figure S4c). Since the ultrathin PS layer was dense and flat, the thickness of the self-assembled block copolymer stripe nanopatterns was calculated to be  $\sim 6$  nm. This result indicates that the block copolymer thin film is a monolayer.

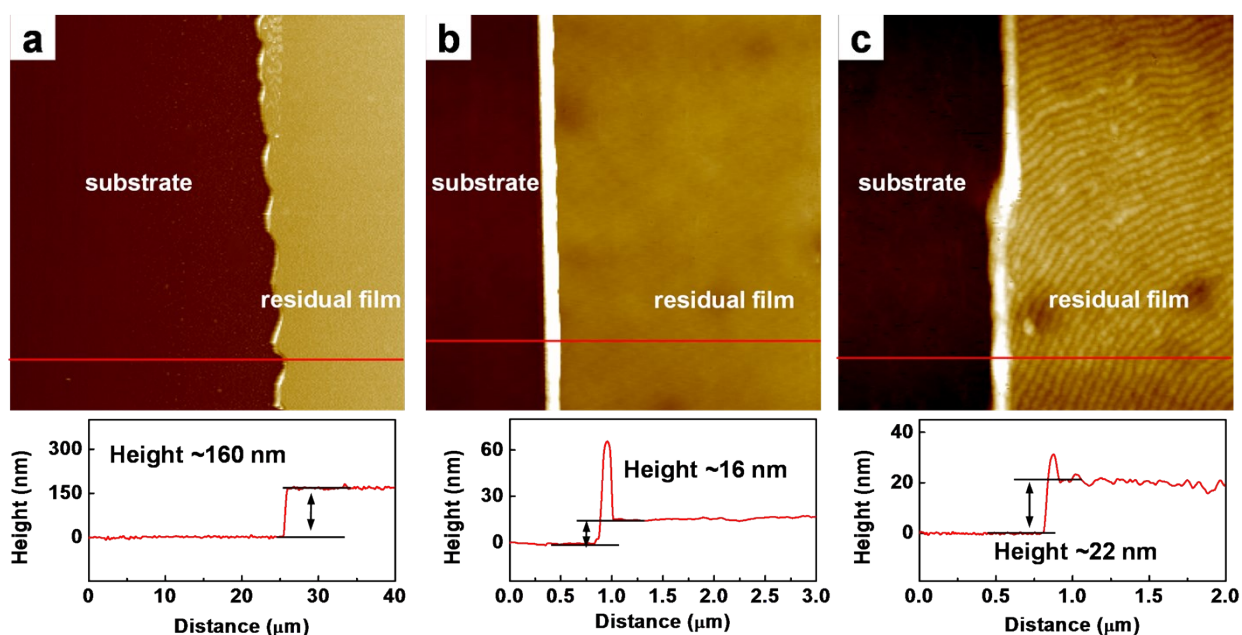


**Figure S4.** AFM topographic images of the height of steps obtained by scratching parts of the organic layers off with a razor blade. (a) Spin-cast PS film,  $40 \mu\text{m} \times 40 \mu\text{m}$ . (b) The resultant ultrathin PS film after heat treatment and toluene rinsing,  $3 \mu\text{m} \times 3 \mu\text{m}$ . (c) The stripe nanopatterns self-assembled on the PS-silicon substrate,  $2 \mu\text{m} \times 2 \mu\text{m}$ .

### 2.3 Self-Assembly of PBLG-*b*-PEG with Higher Molecular Weights on Substrate

For the self-assembly of PBLG-*b*-PEG block copolymers with high PBLG molecular weights on the PS-silicon substrate, disordered structures were obtained. Figure S5 shows the morphologies self-assembled from PBLG<sub>66k</sub>-*b*-PEG<sub>5k</sub> (~92.9 wt% PBLG) on the surface of the PS-silicon wafer. The block copolymers show a propensity to form dispersed nanofibers on the substrate. The  $M_n$  of PBLG block is 66 kg mol<sup>-1</sup> and the resulting nanofibers have a width of ~90 nm.

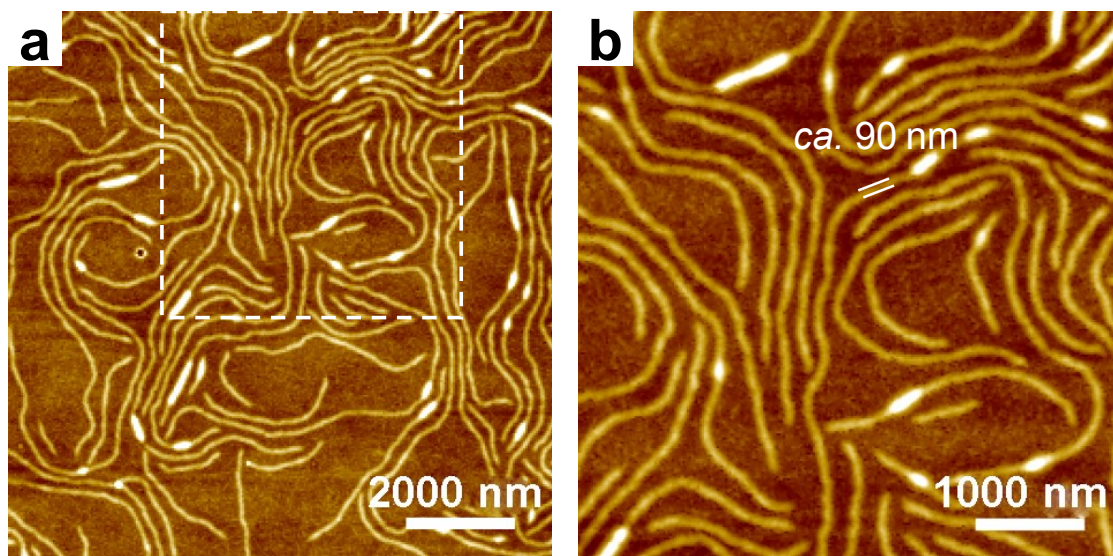


**Figure S5.** (a) AFM image of the nanofibers self-assembled from PBLG<sub>66k</sub>-*b*-PEG<sub>5k</sub> block copolymers on the PS-silicon substrate. (b) Close-up AFM image of the nanofibers shown in the dashed square region of (a).

## 2.4 Self-Assembly of Rod-Coil Copolymers on Substrate Revealed by Simulations

In DPD simulations, a model containing a planar substrate and  $R_4C_4$  (R for rigid PBLG and C for flexible PEG) rod-coil block copolymers was constructed to represent the hydrophobic PS-silicon substrate and the amphiphilic PBLG-*b*-PEG copolymers, respectively. Details about the simulations are provided in Section 1.3 of the Supporting Information. In the initial state, the rod-coil diblock copolymers were randomly distributed in the simulation box. After the simulations were performed for 20000  $\tau$ , the diblock copolymers formed well-aligned stripe patterns on the planar substrate, as shown in Figure S6a. The cross-sectional image of the stripe patterns reveals that the stripes are “semi-cylinder” surface micelles where the rod blocks form the inner cores that are wrapped by the coils. The rod blocks are packed in a “head-to-head” fashion (Figure S6b).

To gain insights into the packing of rod blocks, we measured the angle between the orientation of rod blocks and the planar substrate. Figure S6c shows the probability distribution of the angle  $\alpha$  versus its degree. As can be seen, there is a decrease in the probability distribution of  $\alpha$  with increasing the  $\alpha$ . It was found that about 34 % of the angles were distributed in the range of 0 ~ 10° and only 1.45 % of the angles were distributed in the range of 80 ~ 90°. This result reveals that rod blocks tend to lie down on the substrate as the hydrophobic rod blocks have a strong affinity to the substrate. Figure S6d shows the average  $\varphi$  varied with the height of stripes H (the definition of  $\varphi$  is presented by the inset). The average  $\varphi$  has a maximum of 62.6° at  $H = 0.1 r_c$ , which means that the rod blocks which are close to the substrate surface tend to be perpendicular to the stripe axis. With increasing the H, the  $\varphi$  decrease to 41.0°. This result indicates that rod blocks attached to the substrate surface tend to be perpendicular to the stripe axis.

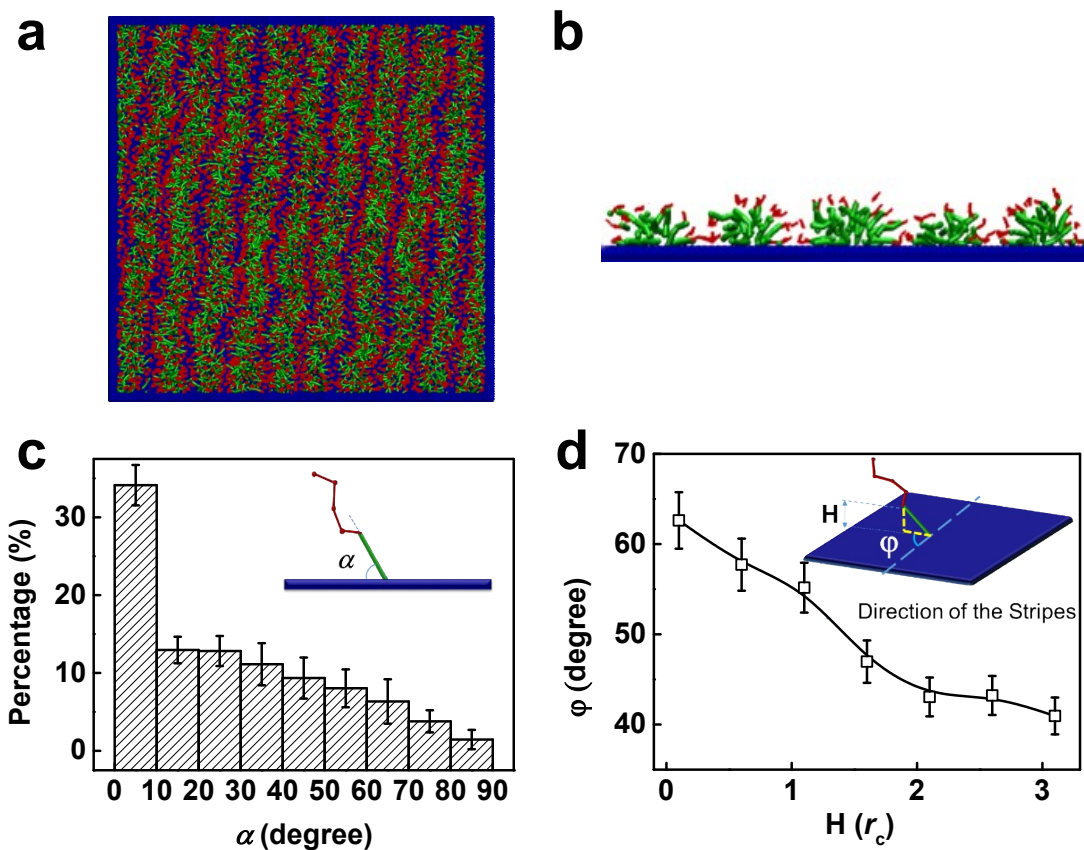


**Figure S6.** (a) Typical stripe patterns calculated by DPD simulations. (b) The side view of the stripe patterns. (c) The probability distribution of the angle  $\alpha$ , the insert shows the schematic illustration of the angle  $\alpha$ . The horizontal and vertical axes indicate values of  $\alpha$  and the percentage of the corresponding angle  $\alpha$ , respectively. (d) The average  $\varphi$  varies with the height of stripes  $H$ . Inset shows a schematic illustration of the angle  $\varphi$  between the orientation of rod blocks and the direction of the stripe patterns.

## 2.5 Aggregates Formed in Solutions at High Block Copolymer Concentrations

When the initial concentration of PBLG-*b*-PEG block copolymer is high (*e.g.*, 1.0 g L<sup>-1</sup>), the adsorption of copolymers on the PS-silicon substrate is saturated, and the excess copolymers are dispersed in the solutions to form small aggregates with the addition of water, as revealed by the TEM image shown in Figure S7.

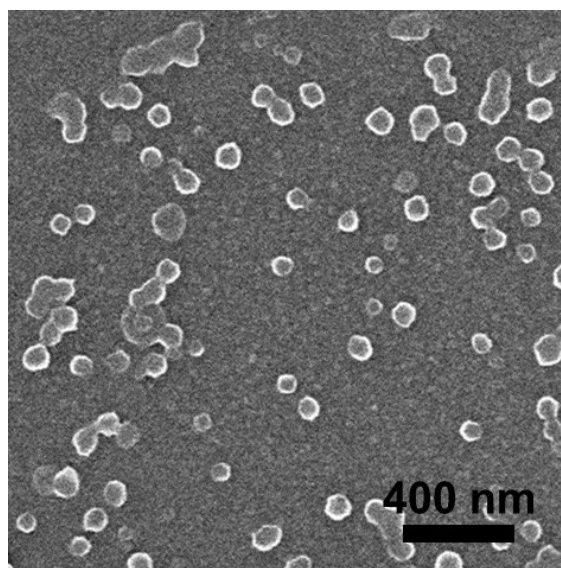


**Figure S7.** TEM image of the spherical aggregates formed by PBLG<sub>12k</sub>-*b*-PEG<sub>5k</sub> block copolymers in solutions with the initial copolymer concentration of 1.0 g L<sup>-1</sup>.

## 2.6 Effect of Assembling Temperature on Surface Morphology

Despite the fact that the stripe morphology is significantly affected by the assembling temperatures, the stripes produced at all the experimental temperatures exhibit a periodic arrangement. As shown in Figure S8, the corresponding 2D GISAXS patterns reveal that the periodicity of the stripe patterns exists over all the experimental temperatures. The apparent scattering spots along the  $xy$ -direction indicate that the stripes are orderly packed along the in-plane direction with a single layer.

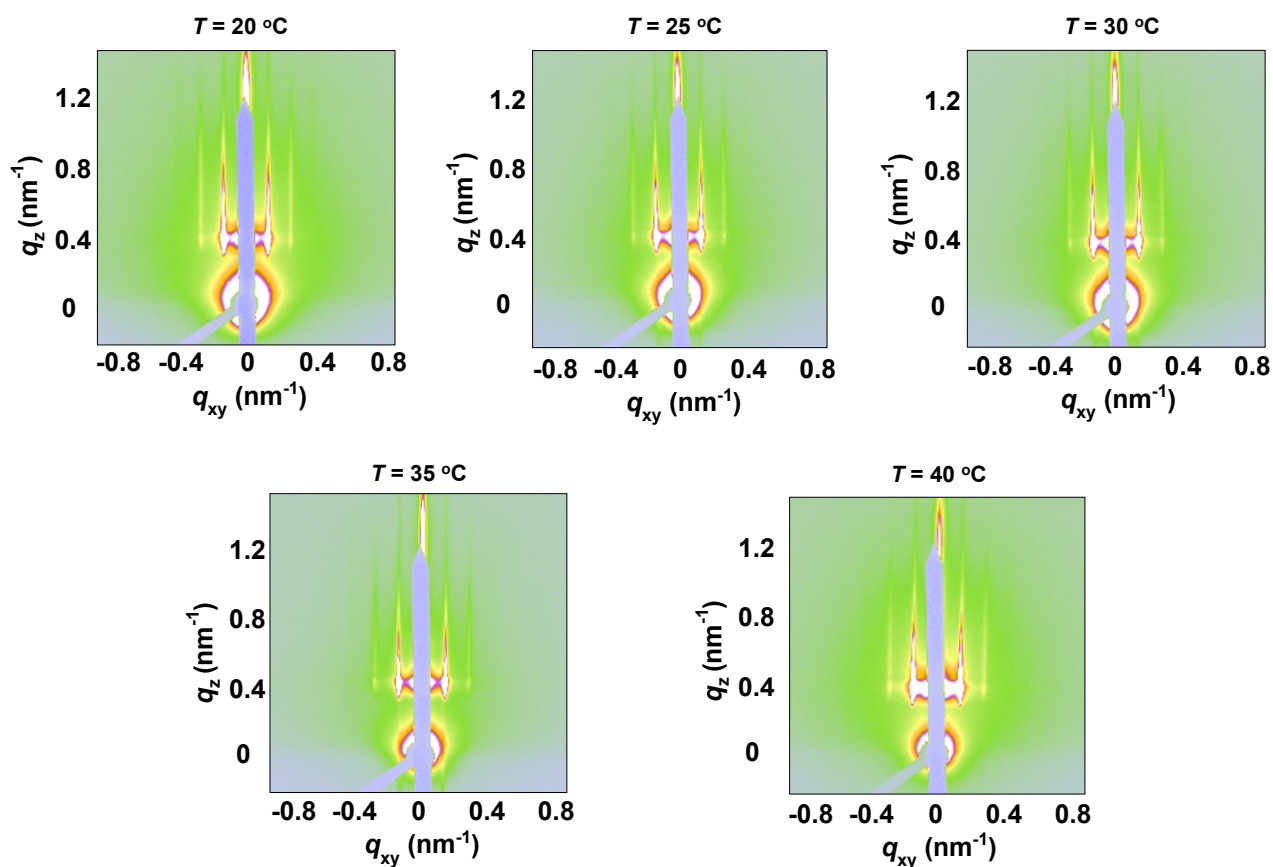


**Figure S8.** 2D GISAXS patterns of the stripe patterns self-assembled at 20 °C to 40 °C.

## 2.7 Effect of THF/DMF Ratios and Temperatures on Surface Morphology

The initial THF/DMF ratios were also found to have an effect on the self-assembled surface morphology. As shown in Figure S9, when the content of DMF is lower, for example, THF/DMF = 7/3 v/v, well-aligned stripe nanopatterns are formed on the PS-silicon substrate. The assembling temperature also influences on the surface morphology, *i.e.*, the stripes swell randomly at higher temperatures. When the DMF content is higher, for example, THF/DMF = 3/7 v/v, the structures formed by PBLG-*b*-PEG on the substrate become disordered (Figure S10). The balance of the interactions between block copolymers and substrates may have a significant influence on the self-assembled morphologies. By changing the experimental conditions, such as initial solvent composition and assembling temperature, the balance of the interactions between polymer chains and the substrate can be changed, resulting in the variation of the final self-assembled nanostructures on the substrate.

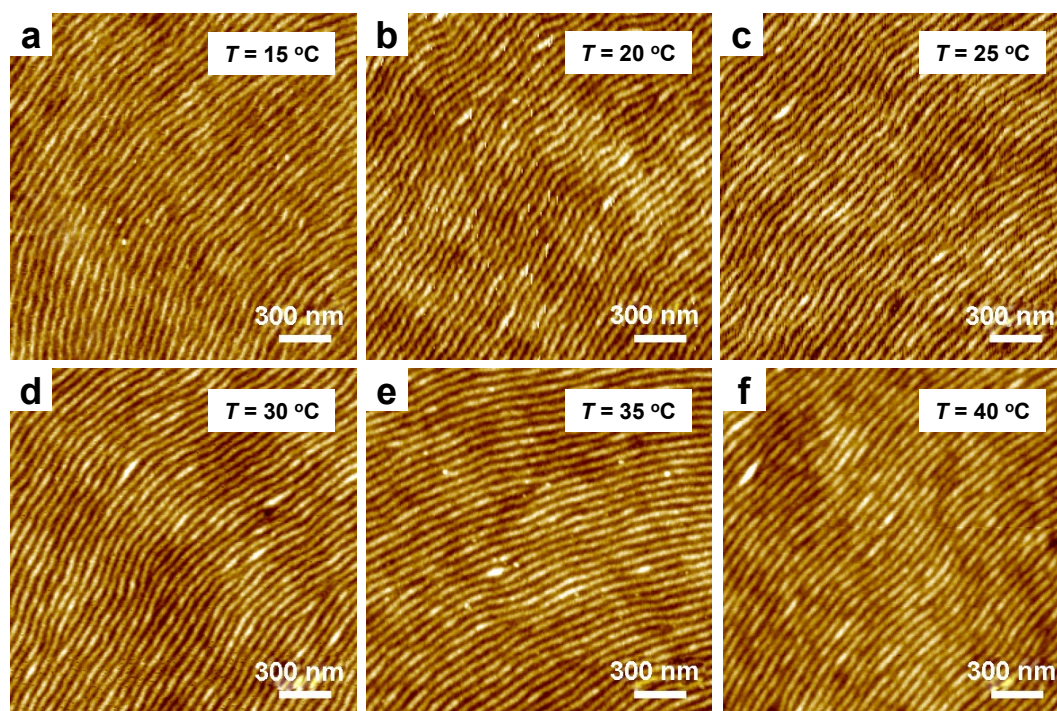


**Figure S9.** AFM images of the stripe nanopatterns self-assembled from various temperatures: (a) 15 °C; (b) 20 °C; (c) 25 °C; (d) 30 °C; (e) 35 °C; (f) 40 °C. The initial solvent is THF/DMF = 7/3 in

volume.

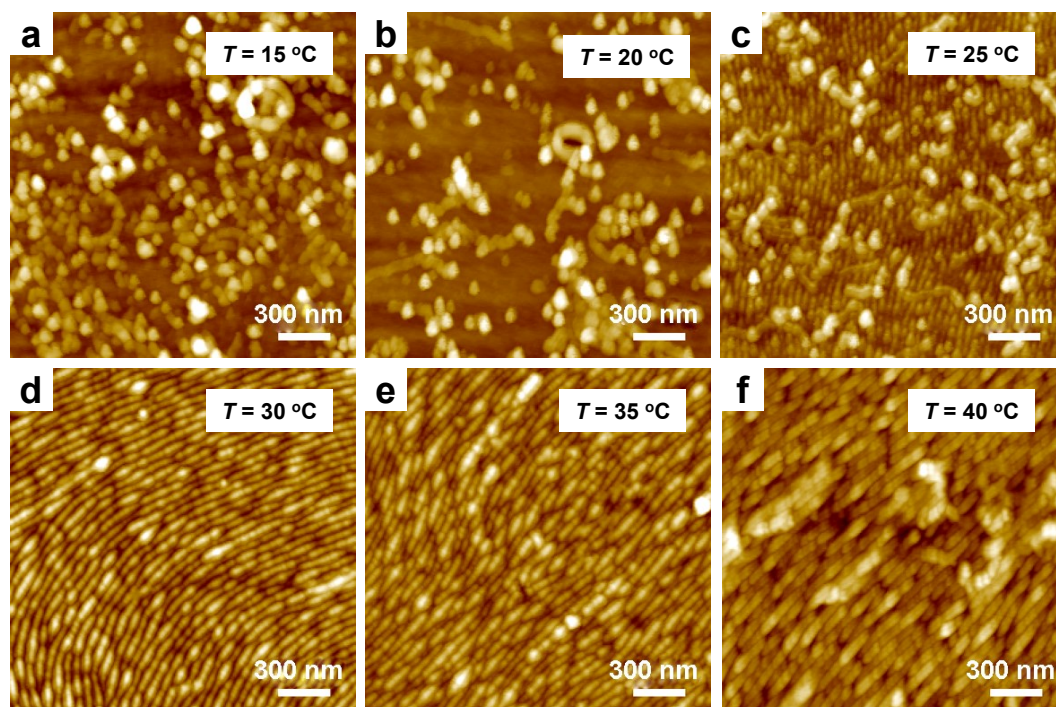


**Figure S10.** AFM images of the surface morphologies self-assembled from various temperatures: (a) 15 °C; (b) 20 °C; (c) 25 °C; (d) 30 °C; (e) 35 °C; (f) 40 °C. The initial solvent is THF/DMF = 3/7 in volume.

## 2.8 Self-Assembly of PBLG-*b*-PEG on Various Substrates

The self-assembly behaviors of PBLG<sub>12k</sub>-*b*-PEG<sub>5k</sub> block copolymers on various substrates were investigated. We firstly prepared a PS-silicon substrate with a clear step-edge between the PS surface and the bared Si substrate (Figure S11a). The height of the step is ~10 nm. Interestingly, it was found that well-aligned stripe nanopatterns are selectively formed on the PS surface, and the orientation of the stripes is nearly parallel to the step-edge (Figure S11b). As compared with the bared Si surface, the hydrophobic PS surface is much more attractive to the block copolymers. As a result, the height of the step changes from ~10 nm to ~16 nm as the block copolymers deposit selectively. Some disordered fibers are also observed in the Si region. This is probably because the surface of the Si region becomes less hydrophilic after heat treatment, and some block copolymers are adsorbed in this region to form aggregates.

We also examined the influence of various polymer-coated substrates on the self-assembled morphology. Two kinds of substrates were prepared, one was the polymethyl methacrylate (PMMA, less hydrophobic) coated substrate, and the other was the poly(2-vinylphridine) (P2VP, hydrophilic) coated substrate. It was found that island-like structures are formed on the PMMA substrate (Figure S11c), which indicates that weaker hydrophobic interactions between the PMMA substrate and the PBLG-*b*-PEG block copolymers are not sufficient for the formation of large-scale continuous nanopatterns. On the other hand, when the hydrophilic P2VP surface was used as the substrate, the block copolymers cannot absorb and assemble on the substrate (Figure S11d). These results indicate that the strong hydrophobic interactions between the substrate and the block copolymers are necessary conditions for the formation of well-aligned stripe nanopatterns. Additionally, the  $\pi$ - $\pi$  interactions between PBLG-PS pairs also contributes the formation and pattern ordering of the film.<sup>[S14]</sup>

Additionally, it should be noted that in the substrate-mediated self-assembly reported in this work, the PS segments on the surface of the PS layer contact with the block copolymers. Therefore, the PS layer thickness does not influence the nanopattern.

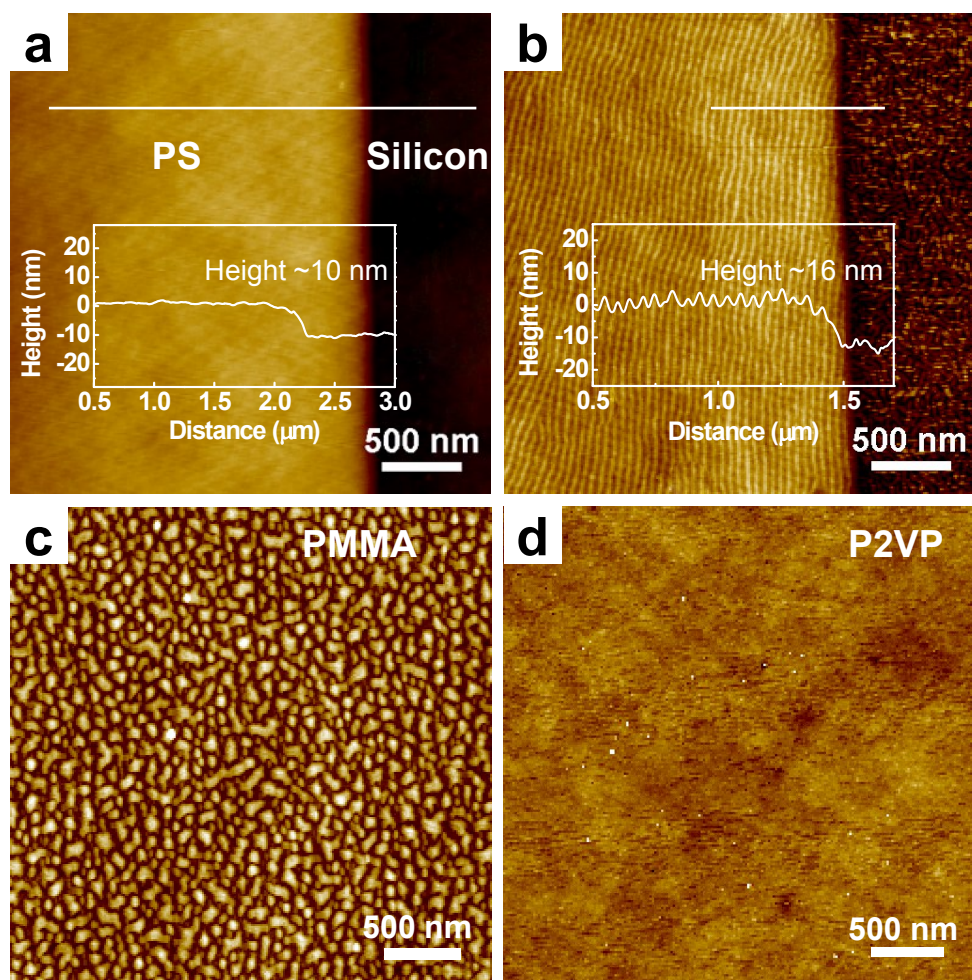


**Figure S11.** (a) A designed PS-silicon substrate with a ~10 nm height step-edge between the PS surface and the bare Si substrate. (b-d) AFM topographic images of the PBLG<sub>12k</sub>-*b*-PEG<sub>5k</sub> block copolymer morphologies self-assembled on various substrates: (b) the specific PS substrate in Figure S11a, (c) PMMA, and (d) P2VP.

## 2.9 Effect of Rigidity of Rod Blocks on Formation of Ordered Nanopatterns

It is noteworthy that the rigid nature of the PBLG blocks is essential to form well-aligned stripe nanopatterns on the substrate. Since PS is a flexible polymer and the interaction between PBLG/PS pairs is comparable to that between PS/PS pairs, we replaced the PBLG<sub>12k</sub>-*b*-PEG<sub>5k</sub> rod-coil block copolymers with PS<sub>15k</sub>-*b*-PEG<sub>5k</sub> coil-coil block copolymers to assemble on the PS-silicon substrate under similar conditions. It was found that PS<sub>15k</sub>-*b*-PEG<sub>5k</sub> can also assemble on the surface of the substrate. However, instead of well-aligned stripe nanopatterns, a rough surface with an irregular pattern on the substrate is formed by the PS<sub>15k</sub>-*b*-PEG<sub>5k</sub> block copolymers (Figure S12). This result indicates that the rigid nature of the PBLG segments is important to generate ordered nanopatterns.

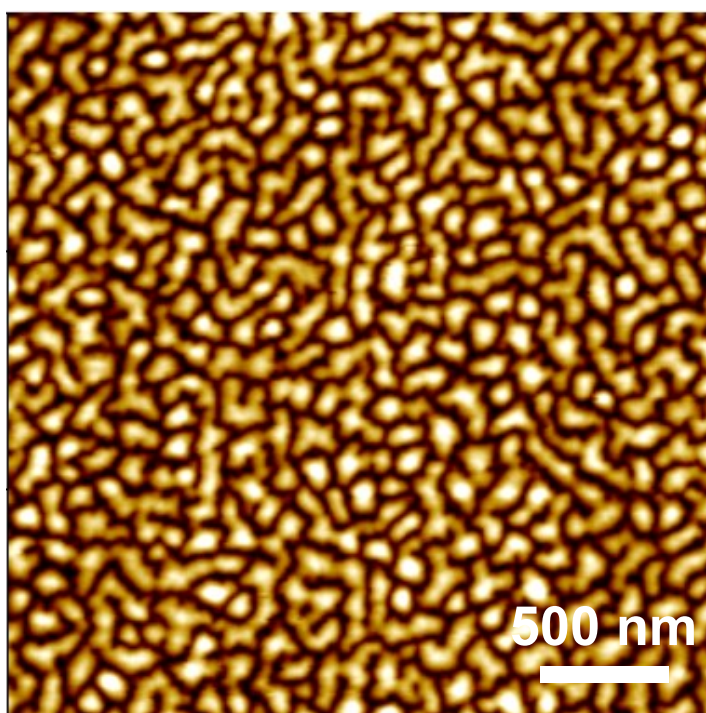


**Figure S12.** AFM image of the structures self-assembled PS<sub>15k</sub>-*b*-PEG<sub>5k</sub> coil-coil block copolymers on the PS-silicon substrate.

## 2.10 Conventional Spin-Coating Approach.

We also performed conventional spin-coating and solvent annealing methods to prepare PBLG-*b*-PEG block copolymer thin films. As shown in Figure S13a, the spin-cast thin films on the PS-silicon substrate show featureless structures. After annealing the films in THF vapor for 48 h, nanofibers are observed. However, it is hard to obtain the ordered structure of polypeptide-based block copolymers, further demonstrating the advantages of adsorption-assembly of PBLG-*b*-PEG block copolymers on the substrate for producing well-ordered nanostructures/nanopatterns.

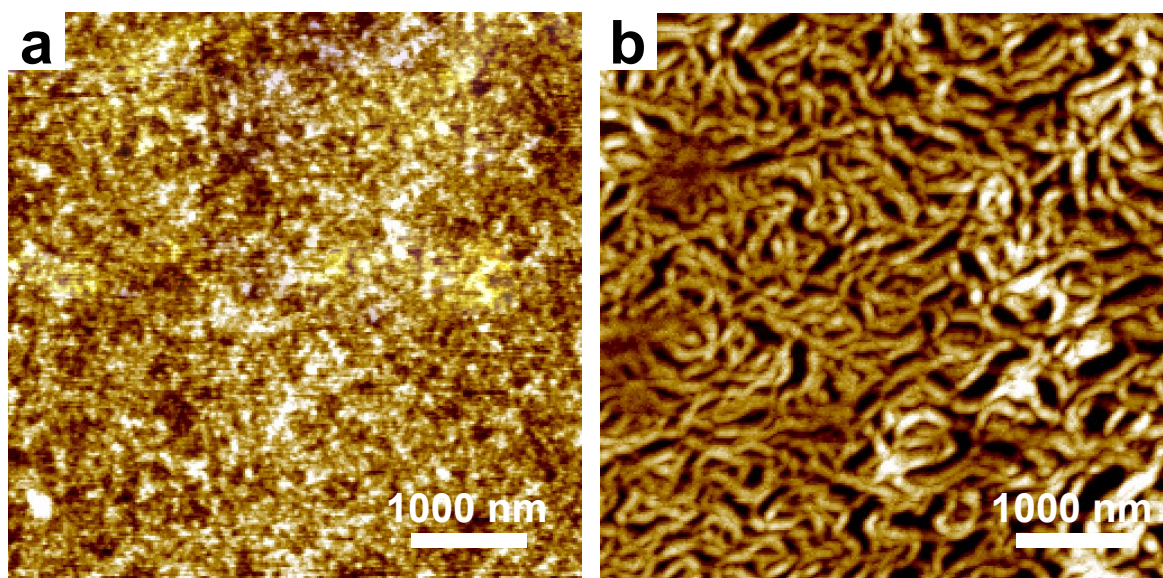


**Figure S13.** AFM images of the films prepared by spin-coating the PBLG<sub>12k</sub>-*b*-PEG<sub>5k</sub> block copolymer solutions onto the PS-silicon substrate. (a) The spin-cast film on the substrate. (b) The structures annealed in THF vapor for 48 h.

## References

- S1. Lin, J.; Abe, A.; Furuya, H.; Okamoto, S. *Macromolecules* **1996**, *29*, 2584-2589.
- S2. Cai, C.; Wang, L.; Lin, J.; Zhang, X. *Langmuir* **2012**, *28*, 4515-4524.
- S3. Cai, C.; Zhu, W.; Chen, T.; Lin, J.; Tian, X. *J. Polym. Sci. Polym. Chem.* **2009**, *47*, 5967-5978.
- S4. Fujii, Y.; Yang, Z.; Leach, J.; Atarashi, H.; Tanaka, K.; Tsui, O. K. C. *Macromolecules* **2009**, *42*, 7418-7422.
- S5. Housmans, C.; Sferrazza, M.; Napolitano, S. *Macromolecules* **2014**, *47*, 3390-3393.
- S6. Nguyen, H. K.; Labardi, M.; Lucchesi, M.; Rolla, P.; Prevosto, D. *Macromolecules* **2013**, *46*, 555-561.
- S7. Ediger, M. D.; Forrest, J. A. *Macromolecules* **2014**, *47*, 471-478.
- S8. Jiang, N.; Shang, J.; Di, X.; Endoh, M. K.; Koga, T. *Macromolecules* **2014**, *47*, 2682-2689.
- S9. Koelman, J. M. V. A.; Hoogerbrugge, P. J. *Europhys. Lett.* **1993**, *21*, 363-368.
- S10. Hoogerbrugge, P. J.; Koelman, J. M. V. A. *Europhys. Lett.* **1992**, *19*, 155-160.
- S11. Groot, R. D.; Warren, P. B. *J. Chem. Phys.* **1997**, *107*, 4423-4435.
- S12. Zhuang, Z.; Jiang, T.; Lin, J.; Gao, L.; Yang, C.; Wang, L.; Cai, C. *Angew. Chem. Int. Ed.* **2016**, *55*, 12522-12527.
- S13. Ding, W.; Lin, S.; Lin, J.; Zhang, L. *J. Phys. Chem. B* **2008**, *112*, 776-783.
- S14. Xu, W.; Xu, Z.; Cai, C.; Lin, J.; Zhang, S.; Zhang, L.; Lin, S.; Yao, Y.; Qi, H. *J. Phys. Chem. Lett.* **2019**, *10*, 6375-6381.